JACS
JOURNAL OF THE AMERICAN CHEMICAL SOCIETY
pubs.acs.org/JACS
Article

# Biosynthetic Lanthanide-Luminescent Mini-Proteins Using Genetic Code Expansion

Edan Habel, Haocheng Qianzhu, Elwy H. Abdelkader, Nathan Paul, Gottfried Otting, and Thomas Huber*

Cite This: J. Am. Chem. Soc. 2026, 148, 14391−14399
Read Online
ACCESS | Metrics & More | Article Recommendations | Supporting Information

**ABSTRACT:** Noncanonical amino acids (ncAA) are promising as light-harvesting antennae for lanthanide luminescence in lanthanide-binding peptides and proteins. Here, we present empirical insights into antenna−lanthanide interactions, which reveal design principles of bright luminescent proteins. Peptides designed to act as lanthanide-binding tags (LBT) show a trade-off between sensitization and lanthanide-binding affinity. We generated a new protein, termed RF2, through computational design with nanomolar binding affinity and more than a 2-fold increase in terbium(III) luminescence relative to LBT. In this scaffold, 6-azatryptophan (6AW) achieved a 10-fold enhancement of the europium(III) luminescence *in vivo*. The RF2 6AW mutant also sensitizes the luminescence of dysprosium(III) and samarium(III). These results demonstrate the capability of *de novo* protein design to produce highly luminescent lanthanide-binding mini-proteins with a genetically encoded ncAA antenna.

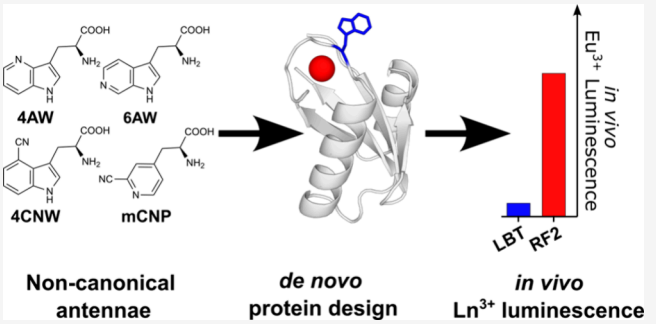




## INTRODUCTION

Lanthanide ions are promising luminescent probes: they exhibit long luminescence lifetimes (0.5−3 ms), large pseudo-Stokes shifts (150−300 nm), and narrow emission bands.[1] These photophysical properties are attractive for time-resolved fluorescence imaging as used with great benefit in immunoassays.[2,3] In biological systems, however, free lanthanides readily precipitate with phosphates and their toxicity warrants strong chelators. Most critically, the molar extinction coefficients of lanthanide ions are extremely low, typically ranging between 0.1 and 10 $M^{-1}$ $cm^{-1}$, which makes direct excitation inefficient. Fortunately, the lanthanide luminescence can be enhanced indirectly through nearby organic chromophores. This phenomenon, known as antenna effect, involves the photoexcitation of the organic chromophore followed by energy transfer to the lanthanide ion, overcoming the problem of low intrinsic absorptivity.

Choosing an optimal antenna is difficult because the energy transfer mechanism is complex. After excitation of the chromophore to the singlet state ($S_1$), lanthanide(III) ($Ln^{3+}$) excitation can occur via multiple pathways.[1] The canonical pathway involves intersystem crossing (ISC) to the long-lived triplet state ($T_1$), which in turn excites the $Ln^{3+}$ ion.[1] Sensitization therefore depends on the ISC efficiency as well as the $T_1$-$Ln^{3+}$ spectral overlap, rather than the more easily measurable absorbance and fluorescence properties of the antenna. In addition, energy transfer is also possible directly from the $S_1$ state to the $Ln^{3+}$ ion, although this mechanism is usually disadvantaged by the short (nanosecond) lifetime of the $S_1$ state.[1] Nonetheless, direct $S_1$ sensitization can be significant when there is strong spectral overlap, which has been explicitly modeled in protein−$Ln^{3+}$ complexes.[4] Crucially, both mechanisms rely on the antenna being in close spatial proximity to the $Ln^{3+}$ ion and overlapping spectral properties. Additionally, $Ln^{3+}$ emission is readily quenched by nearby water molecules, necessitating the exclusion of inner-sphere waters to achieve appreciable emission, even when other factors are favorable.[5] Given these intertwined variables, predicting an antenna's performance *a priori* is challenging, prompting the present empirical approach to identify effective sensitizers.

Peptidic lanthanide-binding tags (LBTs), developed by Imperiali and co-workers,[6−12] are biological lanthanide chelators with high specificity and affinity to lanthanide ions. They were specifically designed to include a tryptophan residue to act as the antenna for terbium(III) ($Tb^{3+}$) excitation, with the backbone carbonyl oxygen of the tryptophan coordinating the lanthanide and the indole ring near the $Tb^{3+}$ ion to efficiently photosensitize the $Tb^{3+}$

Received: January 22, 2026
Revised: March 20, 2026
Accepted: March 23, 2026
Published: March 31, 2026





https://doi.org/10.1021/jacs.6c01416
J. Am. Chem. Soc. 2026, 148, 14391−14399

luminescence. Additional carboxyl groups from acidic side chains and carbonyls from amide-containing side chains prevent the direct access of water to the lanthanide ion, enhancing the luminescence lifetimes and integrated emission intensities. Among the canonical amino acids, tryptophan (Trp) has the highest molar absorption coefficient (~5500 $M^{-1}$ $cm^{-1}$ at 280 nm) and provides the best antenna. Tyrosine (Tyr) in this position has also been established to sensitize the $Tb^{3+}$ luminescence. Complexes using Trp/Tyr antennae are weaker with $Ln^{3+}$ ions other than $Tb^{3+}$,[13,14] as these ions are more effectively quenched by inner-sphere water than $Tb^{3+}$.[15] Besides water quenching effects, differences between complexes reflect energy-level matching of the antennae to the emitting ion.[16]

Over the past decade, there has been increasing interest in biosynthetic molecules to detect, isolate, and utilize lanthanides. In 2018, lanmodulin, a protein from a lanthanide-utilizing bacterium, was identified to have picomolar affinity for lanthanide ions.[17] Lanmodulin, which is structurally analogous to calmodulin, presents a lanthanide chelating environment similar to the LBTs with one residue coordinating the lanthanide ion by a backbone carbonyl oxygen. Featherston et al. reported that mutation of this amino acid to tryptophan sensitizes a $Tb^{3+}$ ion for excitation at 280 nm.[18] Further studies with luminescent lanthanide-binding proteins and peptides have been reviewed by Pazos and coworkers.[19] However, few attempts have been made to generate new lanthanide-binding peptides or proteins explicitly for optimal luminescence properties.

Substituting canonical amino acids by chemically synthesized antenna has been shown to allow for different lanthanide ions to be excited. Reynolds et al. used solid-phase peptide synthesis to substitute a tryptophan with a noncanonical amino acid (ncAA) containing either an acridone or carbostyril side chain. This enhanced the excitation of europium(III) ($Eu^{3+}$) luminescence and, with acridone, the luminosity of $Tb^{3+}$.[9] Other peptide-based lanthanide-luminescent probes were synthetically modified to include a fluorescent moiety,[20−23] although this approach tends to increase the distance between the antenna and the lanthanide ion. All of these peptides require specific chemical synthesis and none can be produced *in vivo*.

Genetic code expansion (GCE) enables the site-specific installation of spectroscopically active ncAAs during protein biosynthesis in *Escherichia coli* by using orthogonal aminoacyl-tRNA synthetase/tRNA pairs with amber stop suppression.[24] We recently expanded the repertoire of genetically encoded tryptophan analogues, opening a modular route to incorporate antennae directly in recombinantly produced polypeptides.[25−28] The present work systematically explores the performance of these ncAAs (Figure 1) as substitutes of Trp at the lanthanide-proximal site.

The ncAAs feature excitation wavelengths in the range 260−350 nm, which proved particularly beneficial for $Eu^{3+}$ sensitization. We analyze the relationship between the antennae and the photoproperties of the $Ln^{3+}$ complexes. Building on the experience gained with LBTs, we computationally designed three new lanthanide-binding mini-proteins. Two of these showed increased luminosity compared to their LBT parents, and one displayed low-nanomolar binding affinity with $Ln^{3+}$ ions. The best-performing antenna was successfully combined with the most tightly binding lanthanide-binding protein, indicating that the luminescence enhancement achieved by the ncAAs is generalizable to other protein scaffolds, providing a basis for new *in vivo* probes.

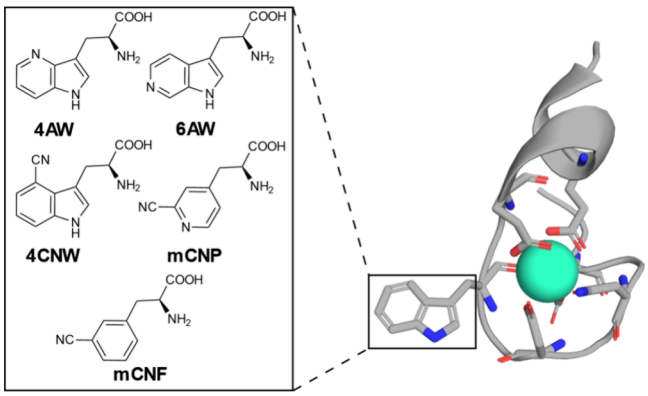


**Figure 1.** Binding geometry of the LBT (PDB ID: 1TJB) with a $Tb^{3+}$ ion bound. The chemical structures are shown for the ncAAs used to substitute the antenna tryptophan, including 4-azatryptophan (4AW), 6-azatryptophan (6AW), 4-cyanotryptophan (4CNW), 3-cyano-4-pyridylalanine (mCNP), and 3-cyanophenylalanine (mCNF).

## RESULTS AND DISCUSSION

All peptides and proteins were produced by recombinant protein expression in *E. coli*. ncAAs were installed using our previously developed two-plasmid system for *in vivo* incorporation of ncAAs via amber stop codon suppression (see Supplementary Methods).[29]

### Enhanced Luminescent Properties with ncAAs

To obtain directly comparable results, we chose the previously reported lanthanide-binding peptide with the sequence GFIDTNNDGWIEGDELLEG for its strong binding affinity and specificity for $Tb^{3+}$, low intrinsic fluorescence, and documented luminescence.[8] The tryptophan at position 10 marks the antenna position, which was modified by ncAAs. For all proteins, successful expression was confirmed by intact protein mass spectrometry (Figures S1−S11). The N-terminal glycine is a remnant of the N-terminal TEV cleavage site used to liberate the peptide following production as a fusion with the solubilizing NT* domain derived from spider silk protein.[29]

Following incorporation of different ncAAs into the LBT, we explored the link between their fluorescence and capacity for luminescence sensitization. The excitation spectra of the LBT ncAA complexes with $Tb^{3+}$ and $Eu^{3+}$ correlated well with the absorbance spectra of each amino acid, confirming that $Ln^{3+}$ excitation was facilitated by the antenna effect (Figures S12 and S13). Unexpectedly, the highly fluorescent 4CNW (fluorescence quantum yield >0.8 compared with ca. 0.15 in Trp)[30] only minimally enhanced the luminescence of $Eu^{3+}$ and delivered weaker integrated $Tb^{3+}$ emission intensities. In contrast, the relatively weakly fluorescent 4AW revealed brighter luminescence intensity with $Tb^{3+}$ than tryptophan and excited $Eu^{3+}$. The best performance was achieved with 6AW, which features an increased fluorescence quantum yield.[28] Compared with Trp, 6AW enhanced the $Tb^{3+}$ luminescence 50% more and excited the $Eu^{3+}$ luminescence more effectively than any of the other antennae studied.

Analyzing the apparent lanthanide dissociation constant $K_D$ of the LBTs, we found that the incorporation of the noncanonical antennae at position 10 in the LBT consistently reduced the binding affinity 2−8-fold (Table 1 and Figure 2).


https://doi.org/10.1021/jacs.6c01416
J. Am. Chem. Soc. 2026, 148, 14391−14399

**Table 1. Luminescence Properties of the LBT-Based $Eu^{3+}$ and $Tb^{3+}$ Complexes[a]**

| antenna | $\lambda_{ex}$ max (nm) | extinction coefficient at $\lambda_{ex}$ max ($M^{-1}$ $cm^{-1}$) | ncAA Quantum yield $\Phi_{S_1}$ | intensity Tb[b] | intensity Eu[a] | apparent $K_D$ ($Tb^{3+}$)[c] (nM) | apparent $K_D$ ($Eu^{3+}$)[c] (nM) | lifetime ($\tau_{Tb}$)[d] | lifetime ($\tau_{Eu}$)[d] |
|---|---|---|---|---|---|---|---|---|---|
| Trp | 280 | 5422 | 0.14[e] | 682 | 5 | 190 ± 40 | N.D. | 2.6 ms | 1.4 ms |
| mCNP | 267 | 1187 | | 630 | 361 | 1300 ± 90 | 490 ± 30 | 2.7 ms | 1.4 ms |
| mCNF | 275 | 843 | | 423 | 50 | 1400 ± 100 | 940 ± 100 | 2.7 ms | 1.4 ms |
| 4AW | 285 | 6272 | 0.01[e] | 728 | 86 | 1100 ± 50 | 580 ± 30 | 1.6 ms | 1.4 ms |
| 4CNW | 290 | 6041 | 0.80[f] | 323 | 5 | 1000 ± 40 | N.D. | 1.5 ms | 0.7 ms |
| 6AW | 260 | 2108 | 0.41[e] | 1072 | 378 | 800 ± 20 | 830 ± 20 | 2.7 ms | 1.4 ms |

[a]N.D. = not determined. [b]Integrated emission intensity for the complex with lanthanide ion measured at the excitation maximum and 545 nm for $Tb^{3+}$ and 615 nm for $Eu^{3+}$. Samples contained 500 nM $Ln^{3+}$ ion with an excess of LBT in 20 mM MOPS pH 7.0, 50 mM KCl. Exact values are reported in Table S2. [c]Apparent $K_D$ values determined by titrating $Ln^{3+}$ (added as $LnCl_3$) into a solution of 500 nM protein in 20 mM MOPS pH 7.0, 50 mM KCl (Figures S14 and S15). The $K_D$ values and error ranges were determined from a nonlinear fit to the Hill equation for three technical replicates (see Supplementary Methods). [d]Lifetime measurements were performed in 20 mM MOPS pH 7.0, 50 mM KCl at 500 nM $Ln^{3+}$ concentration. $\tau_{Ln}$ was determined by a nonlinear fit of a single-exponential decay to lifetime measurements. The error for these measurements was <0.01 ms. [e]From Abdelkader et al.,[28] measured in PBS. [f]From Qianzhu et al.,[30] measured in PBS.

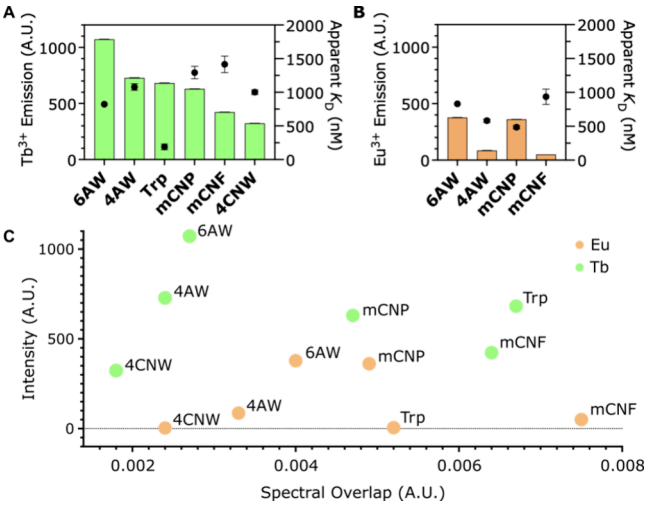


**Figure 2.** Luminescence properties of LBT variants. The histograms show the integrated emission intensities following excitation at the absorption maxima, which were 265 nm for 6AW, 285 nm for 4AW, 280 nm for Trp, 267 nm for mCNP, 275 nm for mCNF, and 290 nm for 4CNW. The binding affinities for these complexes are indicated by black points, which correlate to the right *y*-axis. (A) $Tb^{3+}$ emission at 545 nm. The apparent $K_D$ value of the reference LBT is greater than reported,[6] which we attribute to different buffer conditions. (B) $Eu^{3+}$ emission at 615 nm. The signal intensity of LBT and LBT 4CNW was too weak to measure the affinity. (C) Plot of observed luminescence intensity versus spectral overlap for the series of LBT complexes. Spectral overlap was calculated as the integral of the scalar product between normalized absorption and emission spectra, with each spectrum area-normalized to 1 (Figures S16–S21).

Given that the amino acid sequence of LBT was selected from a large peptide library using $Tb^{3+}$ luminescence,[8] it is unsurprising that even minor side chain modifications can reduce the ion affinity. In contrast, acridone and carbostyril side chains installed in a similar LBT have been reported to perturb binding less (34 nM compared to 19 nM for the wild type).[9] In our experiments, the $K_D$ values differed up to 2.5-fold between $Tb^{3+}$ and $Eu^{3+}$, indicating extreme sensitivity of the lanthanide affinity toward optimal coordination geometry. While the nominal ionic radius differs by only 0.02 Å between $Tb^{3+}$ and $Eu^{3+}$,[31] the effect may result from the nonisotropic electron densities of lanthanide ions.[32,33]

Substituting the antenna with the less fluorescent mCNP greatly enhanced the $Eu^{3+}$ luminescence with little altered enhancement of the $Tb^{3+}$ emission. We speculated that the pyridine nitrogen of the mCNP amino acid directly coordinates the lanthanide ion, thus minimizing the interatomic distance between the antenna and the lanthanide ion. To test this hypothesis, we incorporated mCNF, which exhibits a fluorescence intensity similar to mCNP but lacks the pyridine moiety. mCNF still enhanced the luminescence of $Eu^{3+}$ but significantly less than mCNP, suggesting that coordination plays a significant role. The dissociation constants in Table 1 support this interpretation. mCNP lends itself to rapid chemical diversification using the biocompatible nitrile-aminothiol arcNAT click reaction to generate a range of different fluorophores,[34,35] which invites future exploration.

Our two most highly fluorescent antennae produced very different outcomes: 6AW was the most effective sensitizer for both $Tb^{3+}$ and $Eu^{3+}$ complexes, while 4CNW, despite its high intrinsic fluorescence, sensitized the luminescence of $Tb^{3+}$ only modestly and hardly sensitized $Eu^{3+}$. We also examined whether spectral overlap between the chromophore emission and $Ln^{3+}$ absorption could predict the sensitization efficiency but found no simple correlation.

Coordination with hydration water efficiently quenches $Ln^{3+}$ luminescence.[36] As the luminescence lifetimes of the $Eu^{3+}$ complexes were consistently 1.4 ms, the number of coordinated water molecules does not change between complexes with different ncAAs. The exception to this was LBT 4CNW, which showed a $Eu^{3+}$ lifetime of 0.7 ms. In contrast, the $Tb^{3+}$ luminescence lifetimes of the complexes with tryptophan analogues substituted at the 4-position (4CNW and 4AW) were significantly shorter (1.5 and 1.6 ms, respectively) than for the complex of the wild-type peptide or the LBT made with other ncAAs, suggesting a greater variation in the number of hydration water molecules coordinating the $Tb^{3+}$ ion. Chemical changes at position 4 of the Trp antenna thus appear to alter the coordination geometry of the $Ln^{3+}$ ion.

Table 1 shows the absence of any simple relationship between the integrated emission intensity and the extinction coefficient or fluorescence quantum yield of the antenna. There was also no correlation with the spectral overlap between the antenna and the lanthanide ion. These findings underscore the complexity of the antenna effect in a peptide context and its dependence not only on chromophore brightness but also geometric and electronic compatibility with the lanthanide. The observation that the same antenna performed differently for $Eu^{3+}$ and $Tb^{3+}$ compromises any


https://doi.org/10.1021/jacs.6c01416
J. Am. Chem. Soc. 2026, 148, 14391−14399

simple generalization across lanthanides. Furthermore, as all ncAAs reduced the binding affinity at least 2-fold, we sought the design of a robust protein scaffold that tolerates antenna modifications without trade-offs in lanthanide-binding affinity.

## Computational Design of Novel Lanthanide-Luminescent Mini-Proteins

To generate new, lanthanide-luminescent mini-proteins by computational design, we used Rosetta,[37] RFDiffusion,[38] and ProteinMPNN.[39] The natural lanthanide-binding protein lanmodulin presents an attractive starting point as it features picomolar binding affinity for $Ln^{3+}$ ions and has been studied in detail.[18,40,41] However, its multiple EF hands produce a concentration-dependent lanthanide-binding stoichiometry, which limits its suitability for a wider range of applications. We therefore used only the EF hand 2 (EF2) of lanmodulin as the starting point of the protein design process. EF2 features a threonine residue with similar backbone carbonyl coordination to the lanthanide as the antenna Trp in LBT.[40] To enable the coordination of the tryptophan carbonyl to the metal, the preceding residue is glycine.[7] It is known that tryptophan substitutions at this position in lanmodulin enable lanthanide excitation without significantly perturbing the $Tb^{3+}$ binding affinity.[18]

Coordinates of the 12 residues of EF2 (DPDKDGTLDAKE) were extracted from the NMR structure (PDB ID: 6MI5).[40] Following mutating Thr7 to tryptophan, we energy minimized the side chain in Rosetta and used the resulting peptide geometry as seed structure input to RFDiffusion, diffusing a 70- or 50-amino-acid protein with both N- and C-terminal extensions to the lanthanide ion binding motif. The generated backbone structures were used as input to ProteinMPNN, yielding eight sequences for each backbone. A $Tb^{3+}$ ion was placed for coordination in the protein and threaded with the ProteinMPNN sequences in Rosetta using the *ref2015* score function.[42] The full details of the design process are reported in the Supporting Information.

Given the absence of explicit activity or binding considerations in RFDiffusion and ProteinMPNN, the scoring only accounted for a known binding geometry. Final structures were visually assessed, considering secondary structure diversity, solvent exposure of the $Ln^{3+}$ ion, and plausible $Ln^{3+}$-O distances. Three unique proteins with the best scores across all our evaluation criteria were chosen for experimental validation and expressed with an N-terminal $His_6$-tag and TEV cleavage site. In the following, these proteins are referred to as RF1, RF2, and RF3.

The three proteins have less than 35% sequence identity to lanmodulin. Using the Alphafold3 Web server,[43] each sequence produced high-confidence structures with a calcium ion bound at the desired site. Each protein was recombinantly expressed in *E. coli*, using autoinduction media, with the gene under a T7 promoter (see the Supplementary Methods). RF1, RF2, and RF3 were isolated by immobilized metal ion chromatography (IMAC), with yields of 10, 400, and 15 mg per liter of cell culture, respectively. RF1 and RF3 not only expressed in much lower yields but were also more prone to precipitation at room temperature compared with the highly expressing RF2 protein.

All three designed proteins (RF1, RF2, and RF3) produced a significant luminescence response when incubated with $Tb^{3+}$ (Table S5). Relative to the reference LBT, the luminescence intensities for RF1 and RF2 represented a 1.8-fold and 2.5-fold enhancement, respectively. In contrast, RF3 showed a diminished intensity of about 70% compared to LBT. The $Tb^{3+}$ affinities followed a similar trend, with RF2 showing the strongest apparent binding affinity at $K_D$ = 19 ± 3 nM, followed by RF1 at 320 ± 50 nM and RF3 at 3300 ± 130 nM. RF1, RF2, and RF3 showed lifetimes of 1.39, 1.45, and 1.30 ms, respectively. All were above 1.2 ms, suggesting effective exclusion of water from the inner coordination sphere of the $Tb^{3+}$ complex.[36] However, the values are shorter than 2.5 ms, which is the typical lifetime of a fully shielded $Tb^{3+}$ complex, implying water is not completely excluded. In summary, all data pointed to RF2 as the most attractive variant, and it was selected for further study.

Figure 3A,B shows the Alphafold3 model of RF2 with a $Ca^{2+}$ ion (Figure 3A). The protein contains two $\alpha$-helices, and one

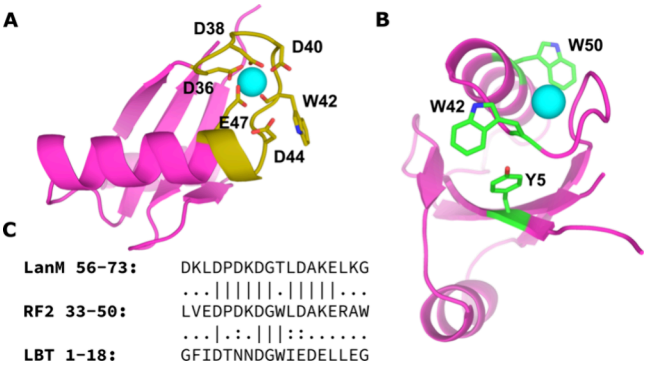


**Figure 3.** AlphaFold3 model of RF2. (A) RF2 model (magenta) with the EF hand highlighted in gold, the $Tb^{3+}$ ion in cyan, and the $Tb^{3+}$ coordinating residues shown in stick representation. (B) Same as (A), but showing RF2 in a different orientation and showing the aromatic residues (green) instead of highlighting the EF hand. (C) Pairwise sequence alignment of lanmodulin EF2, RF2, and LBT with their flanking residues.

$\beta$-sheet comprised of four $\beta$-strands. The EF hand is positioned between $\beta$-strand 3 and $\alpha$-helix 1. Trp42 is placed in the antenna position with the backbone carbonyl coordinated to the ion. A second aromatic amino acid, Tyr5, almost contacts Trp42 (Figure 3B). The presence of Tyr5 may be beneficial, as tyrosine excited at 280 nm can also excite lanthanide luminescence. In principle, the more distant Trp50 may also enhance the antenna effect. These two amino acids introduced by the sequence design of ProteinMPNN may help to produce a stable protein, and we therefore retained them.

To confirm the modeled structure, we prepared a $^{15}N/^{13}C$-labeled sample of RF2 using $^{15}N$-labeled ammonium chloride and $^{13}C$-labeled glucose. The protein was isolated using IMAC with a yield of 100 mg purified protein per liter cell culture. Using 2D and 3D NMR experiments recorded on an 800 MHz NMR spectrometer, we assigned the backbone chemical shifts (C, $C_\alpha$, $C_\beta$, N, H, $H_\alpha$, and $H_\beta$) of most of the 71 amino acids in the protein complexed with yttrium ($Y^{3+}$; Figures S22 and S23). Resonances of residues 10−14 could not be assigned. The backbone dihedral angles $\varphi$ and $\psi$ derived from the chemical shifts by the program TALOS+[44] closely aligned with the Alphafold3 model (Figure S24).

## Enhanced Brightness and More Robust Binding Affinity with an ncAA Antenna

We next tested if the increase in $Eu^{3+}$ luminescence in LBT afforded by ncAAs is transferable to our designed protein. Replacing Trp42 with our best-performing noncanonical


https://doi.org/10.1021/jacs.6c01416
J. Am. Chem. Soc. 2026, 148, 14391−14399

amino acid, 6AW, we compared RF2 6AW with its wild-type parent RF2. The same two-plasmid system as used for LBT expression yielded 56 mg of RF2 6AW per 1 L of cell culture.

Unlike LBT 6AW, RF2 6AW ($\lambda_{ex}$ = 260 nm) showed no significant increase in $Tb^{3+}$ luminescence relative to unmodified RF2 ($\lambda_{ex}$ = 280 nm). We speculate that RF2 features an unusually high brightness owing to additional sensitization by Tyr5 and possibly Trp50, which are excited to a lesser extent at the absorption maximum of 6AW. In contrast, RF2 6AW showed a significant enhancement of $Eu^{3+}$ luminescence, with the excitation spectrum showing increased excitation around 280 nm, relative to LBT 6AW (Figure S25). As the emission maxima for Tyr and Trp are at 304 and 350 nm, respectively, and 6AW possesses a second broad excitation band between 300 and 360 nm (Figures S12), a nonradiative energy transfer from the nearby Tyr and Trp residues to 6AW can arguably add to the enhancement of the $Eu^{3+}$ emission. A mutant with 6AW in position 50 and Trp retained at position 42 showed a decrease in $Tb^{3+}$ excitation, and a minimal increase in $Eu^{3+}$ excitation, suggesting that there is some sensitization from position 50 (Table 2).

**Table 2. Luminescence Properties of the RF2 $Eu^{3+}$ and $Tb^{3+}$ Complexes[a]**

| positions | intensity Tb[b] | intensity Eu[b] | $K_D$ ($Tb^{3+}$)[c] | $K_D$ ($Eu^{3+}$)[c] |
|---|---|---|---|---|
| Trp42/Trp50 | 1784 | <1 | 19 ± 3 nM | N.D.[a] |
| Trp42/6AW50 | 1507 | 13 | 37 ± 5 nM | N.D.[a] |
| 6AW42/Trp50 | 1700 | 506 | 180 ± 12 nM | 150 ± 12 nM |

[a]N.D = not determined. [b]Integrated emission intensity for complex with lanthanide ion measured at the excitation maximum for the antenna and observed at emission wavelengths of 545 nm for $Tb^{3+}$ and 615 nm for $Eu^{3+}$. Samples contained 500 nM $Ln^{3+}$ ion with an excess of RF2. Variants were excited at their excitation maxima, 280 nm for Trp42/Trp50 and Trp42/6AW50, and 260 nm for 6AW42/Trp50. [c]Apparent $K_D$ were measured by titration of $Ln^{3+}$ into a solution of 500 nM protein in 20 mM MOPS pH 7.0, 50 mM KCl (Figure S28). $K_D$ values and error ranges were determined from a nonlinear fit to three technical replicates.

Next, we measured the binding affinity of RF2 6AW with $Tb^{3+}$ and $Eu^{3+}$ and found that the ncAA affects the $Ln^{3+}$ binding affinity by less than an order of magnitude (Table 2). 6AW at position 50 decreases the binding affinity only 2-fold, whereas 6AW at position 42 decreases the affinity almost 10-fold. As in the case of the LBT, the binding affinities differed between $Eu^{3+}$ and $Tb^{3+}$ (Table 2). Nonetheless, even the reduced binding affinities are in the nanomolar range, making the RF2 6AW construct suitable for a wide range of sensing applications.

Encouraged by the excellent enhancement of $Eu^{3+}$ luminescence of RF2 6AW and its nanomolar binding affinities to $Eu^{3+}$ and $Tb^{3+}$, we recorded emission spectra with other trivalent lanthanide ions, including cerium, praseodymium, neodymium, samarium ($Sm^{3+}$), gadolinium, dysprosium ($Dy^{3+}$), erbium, thulium, and ytterbium. We identified weak, but significant, emission peaks with $Sm^{3+}$ and $Dy^{3+}$, which overlapped with the long-wavelength end of the emission peak from 6AW (Figure S27). While the $Sm^{3+}$ emission was too weak for affinity titrations, we were able to determine the apparent $K_D$ value for $Dy^{3+}$ (Figure S28) as 290 ± 30 nM, which corresponds to an only slightly weaker affinity than for $Eu^{3+}$ or $Tb^{3+}$.

To determine the number $q$ of water molecules coordinated to the lanthanide ions, we compared luminescence lifetime measurements in $H_2O$ and $D_2O$ and used the modified Horrocks equation (Figures S29−S32).[36] Empirical correlation coefficients of luminescence quenching by $H_2O$ have been published for $Tb^{3+}$ and $Eu^{3+}$,[36] as well as for $Dy^{3+}$ and $Sm^{3+}$.[45] All four $D_2O$ titrations showed a clear linear response to the percentage of $D_2O$ (Figure S33), yielding $q$-values of 1.07, 1.06, 1.30, and 1.31 for $Tb^{3+}$, $Eu^{3+}$, $Sm^{3+}$, and $Dy^{3+}$, respectively. In view of the inherent uncertainty of this equation of ±0.3 for $Tb^{3+}$ and $Eu^{3+}$, and ±0.5 for $Dy^{3+}$ and $Sm^{3+}$,[45] this indicates that the $Ln^{3+}$ ion in the RF2 complex coordinates a single water molecule. With $q$-values close to 1 across $Tb^{3+}$, $Eu^{3+}$, $Sm^{3+}$, and $Dy^{3+}$, inner-sphere hydration (and thus OH-mediated quenching) varies only little between different lanthanide ions and ncAAs, allowing the brightness and apparent affinity trends to be attributed primarily to the antenna identity.

Two recent studies illustrate alternative strategies in lanthanide-luminescent protein design. A 2023 study grafted a $Tb^{3+}$-binding EF hand into a *de novo* immunoglobulin-like scaffold using ProteinMPNN, yielding a $Tb^{3+}$ affinity of 8−12 μM by time-resolved luminescence.[46] This establishes a *de novo* lanthanide-luminescent protein, but the moderate affinity limits its use under dilute or competitive conditions. More recent work focused on antenna modification, identifying acridone as a strong $Eu^{3+}$ antenna if installed by GCE at three EF hand positions of lanmodulin.[47] Besides involving multiple antenna sites and four additional mutations, the construct leading to $Ln^{3+}$ stoichiometries greater than 1:1 compromises the analysis of antenna performance and lanthanide binding.

## New Lanthanide-Luminescent Mini-Protein Shows Remarkable Selectivity and *In Vivo* Sensitization

Lanthanide ions have high charge density and bind promiscuously to anionic cellular components, including phospholipids,[48] nucleic acids,[49] metal-chelating proteins,[50] and organic phosphates.[51] Lanmodulin has been used as an *in vivo* reporter for lanthanide cellular uptake using a Förster resonance energy transfer (FRET) pair of fluorescent proteins fused to its N- and C-termini, without utilizing the antenna effect.[52] Using FRET rather than the long-lived $Ln^{3+}$ emission prohibits time-gated experiments, which reliably increases sensitivity against background. Quantitative measurements of intracellular $Y^{3+}$ by inductively coupled plasma-mass spectrometry (ICP-MS) reported 3.4 mM of 20 mM $Y^{3+}$ in *E. coli* cells.[41] A recent report showed that free lanthanides adhere strongly to *E. coli* outer membranes,[53] suggesting that the ICP-MS experiments have been compromised by extracellular membrane-bound $Y^{3+}$. Measurements of intracellular lanthanide ion concentrations by luminescence need to take into account the nonspecific binding of $Ln^{3+}$ ions to DNA, which produces UV-excited luminescence.[54] To harness the sensitivity of luminescent detection, any sensor thus needs to bind $Ln^{3+}$ ions with high affinity while affording superior sensitivity. We therefore tested the RF2 scaffold for maintaining its luminescence signal in the face of competing cellular ligands and metal ions.

To investigate the utility of RF2 as a general intracellular lanthanide sensor, we measured the decrease in observable luminescence in the presence of a competing metal ion,[55]


https://doi.org/10.1021/jacs.6c01416
J. Am. Chem. Soc. 2026, 148, 14391−14399

where the binding of various metal ions was evaluated by measuring the change in the sensitized luminescence of a solution containing the RF2/$Tb^{3+}$ complex after the addition of an equimolar amount of competing metal ion. The remaining fraction of initial $Tb^{3+}$ luminescence was used to determine the relative affinity of the competitor, with a fraction of ca. 0.5 indicating a binding affinity comparable to that of $Tb^{3+}$, a fraction <0.5 indicating a stronger affinity, and a fraction >0.5 weaker binding.

The results for competing lanthanide ions were consistent with expectations based on previous titration experiments with RF2 6AW (Figure S28). The addition of $Eu^{3+}$ resulted in a $Tb^{3+}$ luminescence fraction of <0.5, while $Dy^{3+}$ yielded a fraction >0.5 (Figure 4A). Along with many of the $Ln^{3+}$ metals,

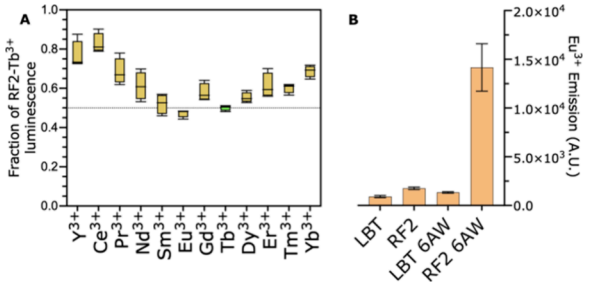


**Figure 4.** (A) Fold change in the luminescence intensity (gold) of RF2 (1 $\mu$M) samples with $Tb^{3+}$ (2 $\mu$M) and competitor (2 $\mu$M) in 20 mM MOPS pH 7.0, 50 mM KCl. Each data point represents the ratio of integrated emission intensity (collected at 545 nm emission with a 100 $\mu$s delay and 1 ms integration window, following excitation at 280 nm) normalized to the intensity of a sample containing only $Tb^{3+}$. The line marked by the green box indicates 50% of the intensity of the RF2/$Tb^{3+}$ complex. Boxes indicate the mean and range of four technical replicates. (B) $Eu^{3+}$ luminescence in *E. coli* B95 cells following overexpression of the protein constructs indicated. The emission values plotted were determined by integration of the emission intensity 600 $\mu$s after excitation at 280 nm and using a 1 ms integration window. Baseline luminescence was subtracted using cells not transformed with the respective plasmid(s) as blanks.

we probed $Ca^{2+}$, $Mg^{2+}$, $Al^{3+}$, and $Fe^{3+}$, which are hard cations like $Ln^{3+}$ ions, and $Zn^{2+}$, $Co^{2+}$. None of these metal ions decreased the $Tb^{3+}$ luminescence at equimolar concentrations, demonstrating their inability to compete for the $Ln^{3+}$ binding site. Unexpectedly, however, $Co^{2+}$ and $Zn^{2+}$ increased the emission intensity at equivalent concentrations (Figure S34), which may indicate the presence of a second metal binding site in RF2 that promotes the luminescence brightness by an allosteric effect. In large excesses of phosphate and ADP (20 mM), we saw a sharp decrease in luminescence, but the $Tb^{3+}$ signal was still observable at 2 $\mu$M (Figure S35). For $Zn^{2+}$, $Ca^{2+}$, and $Mg^{2+}$, the $Tb^{3+}$ luminescence decreased by ~30% at 10,000-fold excess of $Zn^{2+}$, $Ca^{2+}$, and $Mg^{2+}$ (Figure S36), at a metal ion concentration of 20 mM. Together, these data indicate that RF2 shows an appreciable preference for $Ln^{3+}$ over competing metal ions and anions, and the largest effects on luminescence required 10,000-fold excess of the competitor. The strong preference for $Ln^{3+}$ ions relative to the $M^{2+}$ ions may be due to the difference in charge density or due to the subtle nonspherical nature of the $Ln^{3+}$ ions fitting the designed pocket better.

Interestingly, our competition assay gives rise to a parabolic trend in affinity across the lanthanide series, which is strongest for $Eu^{3+}$ and $Tb^{3+}$, with diminishing affinities toward both the heavier and lighter elements (Figure 4A). A similar curve has been reported for LBT,[7] and a minor deviation from the trend for $Gd^{3+}$ has also been reported for both LBT and lanmodulin.[7,55] The sensitivity to lanthanide identity afforded by the *de novo* RF2 mini-protein suggests the potential to design proteins with refined selectivity, which would constitute an important step toward biocompatible alternatives to current metal separation technologies.

In view of the selectivity of RF2 for $Ln^{3+}$ over potential competitors found in biological matrices, we further tested its utility for detecting $Ln^{3+}$ ions in the cytosol of *E. coli* cells. A culture of *E. coli* B95 cells was transformed with the dual-plasmid system. One plasmid encoded either the reference LBT, amber-LBT, or RF2 gene with an amber stop codon at either position 42 or 50. The second carried the orthogonal tRNA/tRNA synthetase pair for the incorporation of 6AW. The cells were grown to $OD_{600}$ of 0.6, and protein expression was induced with 1 mM IPTG. After overnight expression, cells were resuspended in a solution of 150 mM NaCl containing 20 mM $Ln^{3+}$ and then washed with 150 mM NaCl. We found that these conditions produced negligible lysis of the *E. coli* cells for the incubation times tested (Figure S37). The presence of the $Tb^{3+}$ and $Eu^{3+}$ complexes in the cells was readily detected (Figure S38). We chose to excite at 280 and 330 nm, which corresponds to the excitation maximum for tryptophan and the second excitation peak for 6AW, respectively. The luminescence of native cells with $Eu^{3+}$ and $Tb^{3+}$ excited at 330 nm featured a notably high background fluorescence due to the lanthanides binding to components in the cytosol that also sensitize their luminescence. Nonetheless, excitation at 280 nm produced strong *in vivo* sensitization in RF2 6AW, exceeding the signal of the other variants 10-fold (Figure 4B). We repeated this experiment with RF2 6AW and $Eu^{3+}$ without washing the cells. Although this significantly increased the background signal, we could still easily discriminate between RF2 6AW cells and untransformed cells down to 40 $\mu$M (Figure S39). While the antenna effect provides a substantial amplification of the $Eu^{3+}$ signal, the *in vitro* competition data suggest that physiological concentrations of competitors attenuate the lanthanide binding considerably. The observation of a clear RF2 6AW-dependent signal *in vivo* is therefore primarily due to the enhanced antenna effect, rather than its high binding affinity. Future in-cell investigations would be necessary to further elucidate this mechanism of sensitization. This high signal-to-background ratio enables single-wavelength, plate-based measurements of intact cells to detect the presence of $Eu^{3+}$ in the cytosol.

## CONCLUSIONS

This study presents new methods for designing genetically encoded, bright, lanthanide-luminescent complexes in *E. coli* cells, leveraging GCE using selected aaRS/tRNA pairs. Our investigation of various antenna amino acids showed that an empirical approach is required for selecting good antenna for a range of lanthanides, because sensitization efficiency cannot be reliably predicted from the photophysical properties of the sensitizing moiety alone.

The computational designs yielded three proteins that all bind and excite $Tb^{3+}$ ions, two of which outperform the reference LBT as a sensitizing complex. Our lead protein, RF2, has high expression levels, strong and specific binding to lanthanides, and enhanced luminosity. These peptides and proteins can be recombinantly produced and excited by a


https://doi.org/10.1021/jacs.6c01416
J. Am. Chem. Soc. 2026, 148, 14391−14399

range of wavelengths (260−350 nm), and they retain their binding behaviors in the complex environment of the cellular cytosol. Besides the more commonly reported luminescence sensitization of $Tb^{3+}$ and $Eu^{3+}$ ions, the genetically encoded RF2 6AW variant also sensitizes $Dy^{3+}$ and $Sm^{3+}$ luminescence.

The characteristics of our novel, lanthanide-luminescent mini-protein extend the range of biological lanthanide applications. The design of $Ln^{3+}$-binding proteins combined with the sensitization of $Ln^{3+}$ by genetically encoded ncAAs opens the door to straightforward analysis of different $Ln^{3+}$ ions in solution, including in intracellular environments.

## ■ ASSOCIATED CONTENT

### Supporting Information

The Supporting Information is available free of charge at https://pubs.acs.org/doi/10.1021/jacs.6c01416.

Experimental procedures for protein expression and purification; mass-spec of proteins produced; UV/vis, fluorescence, and NMR spectra; equations for calculated values; titrations; and analysis of secondary structures calculated from chemical shifts (PDF)

## ■ AUTHOR INFORMATION


### Corresponding Author

**Thomas Huber** − *Research School of Chemistry, Australian National University, Canberra, ACT 2601, Australia;* orcid.org/0000-0002-3680-8699; Email: t.huber@anu.edu.au

### Authors

**Edan Habel** − *Research School of Chemistry, Australian National University, Canberra, ACT 2601, Australia;* orcid.org/0009-0007-9215-8225

**Haocheng Qianzhu** − *Research School of Chemistry, Australian National University, Canberra, ACT 2601, Australia;* orcid.org/0000-0002-7546-4411

**Elwy H. Abdelkader** − *ARC Centre of Excellence for Innovations in Peptide & Protein Science, Research School of Chemistry, Australian National University, Canberra, ACT 2601, Australia;* orcid.org/0000-0002-5388-3949

**Nathan Paul** − *Research School of Chemistry, Australian National University, Canberra, ACT 2601, Australia;* orcid.org/0009-0009-6370-3196

**Gottfried Otting** − *ARC Centre of Excellence for Innovations in Peptide & Protein Science, Research School of Chemistry, Australian National University, Canberra, ACT 2601, Australia;* orcid.org/0000-0002-0563-0146

Complete contact information is available at: https://pubs.acs.org/10.1021/jacs.6c01416


### Notes

The authors declare no competing financial interest.

## ■ ACKNOWLEDGMENTS

The authors acknowledge the ANU Joint Mass Spectrometry Facility, the ANU Magnetic Resources Facility, and the ANU Biopolymer facility. Financial support by the Australian Research Council for project funding (DP230100079, DP240100273, and CE200100012) is gratefully acknowledged.

## ■ ABBREVIATIONS

aaRS aminoacyl-tRNA synthetase
GCE genetic code expansion
IMAC immobilized metal ion chromatography
IPTG isopropyl β-D-1-thiogalactopyranoside
ncAA noncanonical amino acid
WT wild-type

## ■ REFERENCES


(1) Bünzli, J.-C. G. On the design of highly luminescent lanthanide complexes. *Coord. Chem. Rev.* **2015**, *293*, 19−47.
(2) Bünzli, J.-C. G. Lanthanide luminescence for biomedical analyses and imaging. *Chem. Rev.* **2010**, *110*, 2729−2755.
(3) Bodman, S. E.; Butler, S. J. Advances in anion binding and sensing using luminescent lanthanide complexes. *Chem. Sci.* **2021**, *12*, 2716−2734.
(4) Bruno, J.; Horrocks, W. D., Jr.; Zauhar, R. J. Europium(III) luminescence and tyrosine to terbium(III) energy-transfer studies of invertebrate (octopus) calmodulin. *Biochemistry* **1992**, *31*, 7016−7026.
(5) Mukherjee, P.; Shade, C. M.; Yingling, A. M.; Lamont, D. N.; Waldeck, D. H.; Petoud, S. Lanthanide sensitization in II−VI semiconductor materials: A case study with terbium(III) and europium(III) in zinc sulfide nanoparticles. *J. Phys. Chem. A* **2011**, *115*, 4031−4041.
(6) Nitz, M.; Franz, K. J.; Maglathlin, R. L.; Imperiali, B. A powerful combinatorial screen to identify high-affinity terbium(III)-binding peptides. *ChemBioChem.* **2003**, *4*, 272−276.
(7) Nitz, M.; Sherawat, M.; Franz, K. J.; Peisach, E.; Allen, K. N.; Imperiali, B. Structural origin of the high affinity of a chemically evolved lanthanide-binding peptide. *Angew. Chem., Int. Ed.* **2004**, *43*, 3682−3685.
(8) Martin, L. L.; Sculimbrene, B. R.; Nitz, M.; Imperiali, B. Rapid combinatorial screening of peptide libraries for the selection of lanthanide-binding tags (LBTs). *QSAR Comb. Sci.* **2005**, *24*, 1149−1157.
(9) Reynolds, A. M.; Sculimbrene, B. R.; Imperiali, B. Lanthanide-binding tags with unnatural amino acids: sensitizing Tb3+ and Eu3+ luminescence at longer wavelengths. *Bioconjugate Chem.* **2008**, *19*, 588−591.
(10) Sculimbrene, B. R.; Imperiali, B. Lanthanide-binding tags as luminescent probes for studying protein interactions. *J. Am. Chem. Soc.* **2006**, *128*, 7346−7352.
(11) Barthelmes, K.; Reynolds, A. M.; Peisach, E.; Jonker, H. R.; DeNunzio, N. J.; Allen, K. N.; Imperiali, B.; Schwalbe, H. Engineering encodable lanthanide-binding tags into loop regions of proteins. *J. Am. Chem. Soc.* **2011**, *133*, 808−819.
(12) Victor, T. W.; O'Toole, K. H.; Easthon, L. M.; Ge, M.; Smith, R. J.; Huang, X.; Yan, H.; Chu, Y. S.; Chen, S.; Gursoy, D.; Ralle, M.; Imperiali, B.; Allen, K. N.; Miller, L. M. Lanthanide-binding tags for 3D X-ray imaging of proteins in cells at nanoscale resolution. *J. Am. Chem. Soc.* **2020**, *142*, 2145−2149.
(13) Allen, J. E.; McLendon, G. L. Tryptophan and tyrosine to terbium fluorescence. *Biochem. Biophys. Res. Commun.* **2006**, *349*, 1264−1268.
(14) Brennan, J. D.; Capretta, A.; Yong, K.; Gerritsma, D.; Flora, K. K.; Jones, A. Sensitization of lanthanides by nonnatural amino acids. *Photochem. Photobiol.* **2002**, *75*, 117−121.
(15) Parker, D.; Fradgley, J. D.; Wong, K. L. The design of responsive luminescent lanthanide probes and sensors. *Chem. Soc. Rev.* **2021**, *50*, 8193−8213.
(16) Latva, M.; Takalo, H.; Mukkala, V.-M.; Matachescu, C.; Rodríguez-Ubis, J. C.; Kankare, J. Correlation between the lowest triplet state energy level of the ligand and lanthanide(III) luminescence quantum yield. *J. Lumin.* **1997**, *75*, 149−169.
(17) Cotruvo, J. A., Jr.; Featherston, E. R.; Mattocks, J. A.; Ho, J. V.; Laremore, T. N. Lanmodulin: A highly selective lanthanide-binding

protein from a lanthanide-utilizing bacterium. *J. Am. Chem. Soc.* **2018**, *140*, 15056−15061.
(18) Featherston, E. R.; Issertell, E. J.; Cotruvo, J. A. Probing lanmodulin's lanthanide recognition via sensitized luminescence yields a platform for quantification of terbium in acid mine drainage. *J. Am. Chem. Soc.* **2021**, *143*, 14287−14299.
(19) Sánchez-Fernández, R.; Obregón-Gómez, I.; Sarmiento, A.; Vázquez, M. E.; Pazos, E. Luminescent lanthanide metallopeptides for biomolecule sensing and cellular imaging. *Chem. Commun.* **2024**, *60*, 12650−12661.
(20) Bonnet, C. S.; Devocelle, M.; Gunnlaugsson, T. Luminescent lanthanide-binding peptides: sensitising the excited states of Eu(III) and Tb(III) with a 1,8-naphthalimide-based antenna. *Org. Biomol. Chem.* **2012**, *10*, 126−133.
(21) Ancel, L.; Gateau, C.; Lebrun, C.; Delangle, P. DNA sensing by a Eu-binding peptide containing a proflavine unit. *Inorg. Chem.* **2013**, *52*, 552−554.
(22) Ancel, L.; Niedzwiecka, A.; Lebrun, C.; Gateau, C.; Delangle, P. Rational design of lanthanide-binding peptides. *C. R. Chim.* **2013**, *16*, 515−523.
(23) Yeung, Y.; Chau, H.; Kai, H.; Zhou, W.; Chan, K. H.; Thor, W.; Charbonnière, L. J.; Zhang, F.; Fan, Y.; Wu, Y.; Wong, K. Near-infrared and visible dual-emitting peptide by modular assembly of nitrobenzoxadiazole and neodymium complexes. *Adv. Opt. Mater.* **2024**, *12*, No. 2302070.
(24) Wang, L.; Brock, A.; Herberich, B.; Schultz, P. G. Expanding the genetic code of *Escherichia coli*. *Science* **2001**, *292*, 498−500.
(25) Abdelkader, E. H.; Qianzhu, H.; Huber, T.; Otting, G. Genetic encoding of 7-aza-L-tryptophan: Isoelectronic substitution of a single CH group in a protein for a nitrogen atom for site-selective isotope labeling. *ACS Sens.* **2023**, *8*, 4402−4406.
(26) Abdelkader, E. H.; Qianzhu, H.; Tan, Y. J.; Adams, L. A.; Huber, T.; Otting, G. Genetic encoding of $N^6$-(((trimethylsilyl)-methoxy)carbonyl)-L-lysine for NMR studies of protein−protein and protein−ligand interactions. *J. Am. Chem. Soc.* **2021**, *143*, 1133−1143.
(27) Qianzhu, H.; Abdelkader, E. H.; Otting, G.; Huber, T. Genetic encoding of fluoro-L-tryptophans for site-specific detection of conformational heterogeneity in proteins by NMR spectroscopy. *J. Am. Chem. Soc.* **2024**, *146*, 13641−13650.
(28) Abdelkader, E. H.; Qianzhu, H.; Huber, T.; Otting, G. Isosteric Engineering of Enzymes: Overcoming activity-stability trade-offs by site-selective CH → N substitutions. *bioRxiv* **2026**.
(29) Abdelkader, E. H.; Otting, G. NT*-HRV3CP: An optimized construct of human rhinovirus 14 3C protease for high-yield expression and fast affinity-tag cleavage. *J. Biotechnol.* **2021**, *325*, 145−151.
(30) Qianzhu, H.; Abdelkader, E. H.; Welegedara, A. P.; Habel, E.; Paul, N.; Frkic, R. L.; Jackson, C. J.; Huber, T.; Otting, G. Rendering proteins fluorescent inconspicuously: Genetically encoded 4-cyano-tryptophan conserves their structure and enables the detection of ligand binding sites. *Angew. Chem., Int. Ed.* **2025**, *64*, No. e202421000.
(31) Shannon, R. D. Revised effective ionic radii and systematic studies of interatomic distances in halides and chalcogenides. *Acta Crystallogr., Sect. A* **1976**, *32*, 751−767.
(32) Valencia, L.; Martinez, J.; Macias, A.; Bastida, R.; Carvalho, R. A.; Geraldes, C. F. X-ray diffraction and 1H NMR in solution: Structural determination of lanthanide complexes of a Py2N6Ac4 ligand. *Inorg. Chem.* **2002**, *41*, 5300−5312.
(33) Jiang, S.-D.; Qin, S.-X. Prediction of the quantized axis of rare-earth ions: The electrostatic model with displaced point charges. *Inorg. Chem. Front.* **2015**, *2*, 613−619.
(34) Abdelkader, E. H.; Qianzhu, H.; George, J.; Frkic, R. L.; Jackson, C. J.; Nitsche, C.; Otting, G.; Huber, T. Genetic encoding of cyanopyridylalanine for in-cell protein macrocyclization by the nitrile−aminothiol click reaction. *Angew. Chem., Int. Ed.* **2022**, *61*, No. e202114154.
(35) Abdelkader, E. H.; Qianzhu, H.; Otting, G.; Huber, T. Biosynthesis and genetic encoding of activated nitriles for fast protein conjugation and tunable fluorogenic labeling. *Chem.* **2025**, *11*, No. 102385.
(36) Beeby, A.; Clarkson, I. M.; Dickins, R. S.; Faulkner, S.; Parker, D.; Royle, L.; de Sousa, A. S.; Williams, J. A. G.; Woods, M. Non-radiative deactivation of the excited states of europium, terbium and ytterbium complexes by proximate energy-matched OH, NH and CH oscillators: An improved luminescence method for establishing solution hydration states. *J. Chem. Soc., Perkin Trans. 2* **1999**, 493−504.
(37) Rohl, C. A.; Strauss, C. E.; Misura, K. M.; Baker, D. Protein structure prediction using Rosetta. *Methods Enzymol.* **2004**, *383*, 66−93.
(38) Watson, J. L.; Juergens, D.; Bennett, N. R.; Trippe, B. L.; Yim, J.; Eisenach, H. E.; Ahern, W.; Borst, A. J.; Ragotte, R. J.; Milles, L. F.; Wicky, B. I. M.; Hanikel, N.; Pellock, S. J.; Courbet, A.; Sheffler, W.; Wang, J.; Venkatesh, P.; Sappington, I.; Torres, S. V.; Lauko, A.; De Bortoli, V.; Mathieu, E.; Ovchinnikov, S.; Barzilay, R.; Jaakkola, T. S.; DiMaio, F.; Baek, M.; Baker, D. De novo design of protein structure and function with RFdiffusion. *Nature* **2023**, *620*, 1089−1100.
(39) Dauparas, J.; Anishchenko, I.; Bennett, N.; Bai, H.; Ragotte, R. J.; Milles, L. F.; Wicky, B. I. M.; Courbet, A.; de Haas, R. J.; Bethel, N.; Leung, P. J. Y.; Huddy, T. F.; Pellock, S.; Tischer, D.; Chan, F.; Koepnick, B.; Nguyen, H.; Kang, A.; Sankaran, B.; Bera, A. K.; King, N. P.; Baker, D. Robust deep learning-based protein sequence design using ProteinMPNN. *Science* **2022**, *378*, 49−56.
(40) Cook, E. C.; Featherston, E. R.; Showalter, S. A.; Cotruvo, J. A. Structural basis for rare earth element recognition by lanmodulin. *Biochemistry* **2019**, *58*, 120−125.
(41) Wu, Q.; Liu, X. L.; Chai, Z. F.; Cheng, K.; Xu, G. H.; Jiang, L.; Liu, M. L.; Li, C. G. Lanmodulin remains unfolded and fails to interact with lanthanide ions in cells. *Chem. Commun.* **2022**, *58*, 8230−8233.
(42) Park, H.; Bradley, P.; Greisen, P., Jr.; Liu, Y.; Mulligan, V. K.; Kim, D. E.; Baker, D.; DiMaio, F. Simultaneous optimization of biomolecular energy functions on features from small molecules and macromolecules. *J. Chem. Theory Comput.* **2016**, *12*, 6201−6212.
(43) Abramson, J.; Adler, J.; Dunger, J.; Evans, R.; Green, T.; Pritzel, A.; Ronneberger, O.; Willmore, L.; Ballard, A. J.; Bambrick, J.; Bodenstein, S. W.; Evans, D. A.; Hung, C. C.; O'Neill, M.; Reiman, D.; Tunyasuvunakool, K.; Wu, Z.; Zemgulyte, A.; Arvaniti, E.; Beattie, C.; Bertolli, O.; Bridgland, A.; Cherepanov, A.; Congreve, M.; Cowen-Rivers, A. I.; Cowie, A.; Figurnov, M.; Fuchs, F. B.; Gladman, H.; Jain, R.; Khan, Y. A.; Low, C. M. R.; Perlin, K.; Potapenko, A.; Savy, P.; Singh, S.; Stecula, A.; Thillaisundaram, A.; Tong, C.; Yakneen, S.; Zhong, E. D.; Zielinski, M.; Zidek, A.; Bapst, V.; Kohli, P.; Jaderberg, M.; Hassabis, D.; Jumper, J. M. Accurate structure prediction of biomolecular interactions with AlphaFold 3. *Nature* **2024**, *630*, 493−500.
(44) Shen, Y.; Delaglio, F.; Cornilescu, G.; Bax, A. TALOS+: A hybrid method for predicting protein backbone torsion angles from NMR chemical shifts. *J. Biomol. NMR* **2009**, *44*, 213−223.
(45) Kimura, T.; Kato, Y. Luminescence study on determination of the hydration number of Sm(III) and Dy(III). *J. Alloys Compd.* **1995**, *225*, 284−287.
(46) Roel-Touris, J.; Nadal, M.; Marcos, E. Single-chain dimers from de novo immunoglobulins as robust scaffolds for multiple binding loops. *Nat. Commun.* **2023**, *14*, 5939.
(47) Wang, J.; Liu, X.; Li, K.; Shi, T.; Xu, Q.; Peng, T.; Huang, Q.; Gao, Z.; Zhou, H.; Lu, W.; Wang, J. Design and evolution of a phosphorescent protein via the proximal encoding of lanthanide and the antenna chromophore. *J. Am. Chem. Soc.* **2025**, *147*, 15205−15215.
(48) Sun, J.; Petersheim, M. Lanthanide(III)−phosphatidic acid complexes: Binding site heterogeneity and phase separation. *Biochim. Biophys. Acta, Biomembr.* **1990**, *1024*, 159−166.
(49) Komiyama, M.; Takeda, N.; Shigekawa, H. Hydrolysis of DNA and RNA by lanthanide ions: mechanistic studies leading to new applications. *Chem. Commun.* **1999**, 1443−1451.


https://doi.org/10.1021/jacs.6c01416
J. Am. Chem. Soc. 2026, 148, 14391−14399

(50) Chen, C.; Zhang, P.; Chai, Z. Distribution of some rare earth elements and their binding species with proteins in human liver studied by instrumental neutron activation analysis combined with biochemical techniques. *Anal. Chim. Acta* **2001**, *439*, 19−27.
(51) Eads, C. D.; Mulqueen, P.; Horrocks, W. D., Jr.; Villafranca, J. J. Characterization of ATP complexes with lanthanide(III) ions. *J. Biol. Chem.* **1984**, *259*, 9379−9383.
(52) Mattocks, J. A.; Ho, J. V.; Cotruvo, J. A., Jr. A selective, protein-based fluorescent sensor with picomolar affinity for rare earth elements. *J. Am. Chem. Soc.* **2019**, *141*, 2857−2861.
(53) Zurier, H. S.; Farinato, R.; Kucharzyk, K. H.; Banta, S.; Buan, N. R. The outer membrane in *Acidithiobacillus ferrooxidans* enables high tolerance to rare earth elements. *Appl. Environ. Microbiol.* **2025**, *91*, No. e0245024.
(54) Jastrzab, R.; Nowak, M.; Skrobanska, M.; Tolinska, A.; Zabiszak, M.; Gabryel, M.; Marciniak, L.; Kaczmarek, M. T. DNA as a target for lanthanide(III) complexes' influence. *Coord. Chem. Rev.* **2019**, *382*, 145−159.
(55) Singer, H.; Drobot, B.; Zeymer, C.; Steudtner, R.; Daumann, L. J. Americium preferred: Lanmodulin, a natural lanthanide-binding protein favors an actinide over lanthanides. *Chem. Sci.* **2021**, *12*, 15581−15587.





https://doi.org/10.1021/jacs.6c01416
J. Am. Chem. Soc. 2026, 148, 14391−14399